

# Crosslinked Epoxies: Network Structure Characterization and Physical–Mechanical Properties

U. M. VAKIL\*<sup>†</sup> and G. C. MARTIN

Department of Chemical Engineering and Materials Science, Syracuse University, Syracuse, New York 13244

## SYNOPSIS

A homologous series of epoxy resins, based on the diglycidyl ether of bisphenol-A, were reacted with stoichiometric quantities of *m*-phenylenediamine (*m*PDA) to form networks with varying crosslink densities. Infrared spectroscopic analyses revealed that the networks were formed predominantly by the epoxy–amine addition reactions with little or no OH-etherification. The ultimate glass transition temperatures were inversely proportional to the epoxy chain mol wt, as predicted by a model based on the assumptions of additivity and redistributivity of free volume. The average mol wt between crosslinks,  $\bar{M}_c$ , determined from the dynamic mechanical shear moduli, agreed to within 15 to 18% with the values predicted by the reaction stoichiometry. The glassy-state modulus did not exhibit any  $\bar{M}_c$  dependence above room temperature, however, the modulus–temperature plot for all the networks exhibited a discontinuity near  $-50^\circ\text{C}$  with a steeper slope below  $-50^\circ\text{C}$  than above it. The change in slope occurred over the same temperature interval as the  $\beta$ -transition temperature of the networks. The discontinuity in the modulus–temperature plot can be attributed to the freezing of the localized motions of the molecular groups responsible for the  $\beta$ -transition. © 1992 John Wiley & Sons, Inc.

## INTRODUCTION

Polymer resins are widely used as adhesives and as matrices in fiber-reinforced composites, with applications in the automotive, aerospace, and marine industries. Among the various types of resins, crosslinked epoxies are used most extensively, primarily because these resins possess good thermal and mechanical properties, are easy to process, and are relatively inexpensive. However, in spite of widespread use in high performance applications, the fundamental network structure–mechanical property relations of crosslinked polymers are not adequately understood. In order to synthesize resin systems with the desired mechanical properties, such as high modulus and high fracture strength, it is essential to understand the role of the polymer microstructure in influencing the resin mechanical properties.

The principal objective of this study was to analyze the mechanical properties and the fracture mechanisms of a series of well-characterized networks. Therefore, the moduli, the yield stresses, and the fracture energies of a series of epoxy resins crosslinked with *m*PDA were determined. The results of various preliminary tests used to characterize the networks are discussed here. The correlations between the network structure, the yield stress, and the fracture mechanisms are described elsewhere.<sup>30</sup>

## EXPERIMENTAL

### Materials

The resins used in this study were a homologous series of epoxies, derived from the condensation reaction of bisphenol-A and epichlorohydrin. All resins were supplied by the Shell Chemical Co. and were used without any further purification. In the text, the resins are designated as Epon 825, 836, 1001F, 1002F, and 1004F, according to the manufacturer's nomenclature. The epoxy equivalent weights

\* Present address: AdTech Systems Research Inc., 1342 North Fairfield Road, Dayton, OH 45432.

<sup>†</sup> To whom correspondence should be addressed.

Journal of Applied Polymer Science, Vol. 46, 2089–2099 (1992)

© 1992 John Wiley & Sons, Inc.

CCC 0021-8995/92/122089-11

**Table I** Physical Properties of Epon Resins

Resin	Average Equivalent Weight (g/eq)	Average Value of $n$	$T_g$ (°C)	Melting Point (°C)
Epon 825	175.0	0.04	-31.7	42.3
Epon 836	314.8	1.02	3.9	12.6
Epon 1001F	544.9	2.64	34.6	42.8
Epon 1002F	648.5	3.37	43.4	49.3
Epon 1004F	883.4	4.67	52.9	60.2

(EEW) of the resins were determined by titration with a standard solution of HBr in acetic acid following the procedure outlined in ASTM-D1652.<sup>1</sup>

The number average mol wt of the resins, calculated from the EEW, varied from 350 g/mol for Epon 825 to 1666 g/mol for Epon 1004F. The resin properties are listed in Table I and the structure is shown in Figure 1. The parameter  $n$  in Figure 1 represents the number of repeat units in the structure of the higher mol wt homologs. For Epon 825, with an EEW of 350 g/mol,  $n \approx 0.04$ , while for the highest mol wt resin, Epon 1004F,  $n \approx 4.67$ .

Each resin was crosslinked with stoichiometric quantities of *m*PDA, which was obtained from the Sigma Chemical Company with a minimum purity of 99.8%. Both the epoxies and the amine were used without further purification.

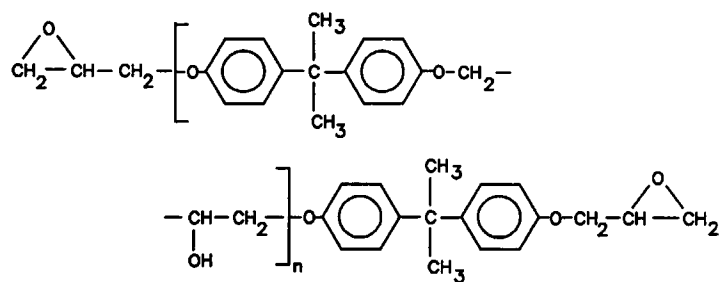
### Cure Procedure

Specimens for the physical and mechanical property characterizations were machined from the cured resin sheets. To prepare the sheets, each resin was first heated to a temperature at which its viscosity was low enough to permit homogeneous mixing. The preheat temperature varied from 70°C for Epon 825 to 185°C for Epon 1004F. The resins were evacuated for 1 to 2 h to remove residual volatiles. The amine was melted independently and then was added to the liquid resin. The mixture was rigorously stirred

for a few minutes and then was poured into preheated aluminum molds coated with a fluoropolymer release agent.

The cure and postcure schedules for the different resins are listed in Table II. Since the objective of the research was to analyze the network structure influence on the mechanical properties, all efforts were made to synthesize "ideal" networks, where each resin chain would be attached to two amine molecules and each amine molecule, in turn, would be linked to four epoxy chains.

The curing mechanisms of epoxy-amine systems have been studied extensively by a number of investigators.<sup>2-6</sup> The principal reactions that occur during the cure of stoichiometric mixtures of epoxy-aromatic amine systems are: (i) the addition of a primary amine to an epoxy to form a secondary amine, and (ii) the addition of a secondary amine generated in step (i) to another epoxy to form a tertiary amine.<sup>5,6</sup> Ideally, reactions (i) and (ii) can generate a three-dimensional network with the epoxy chains end-linked by the amine molecules. However, a third reaction, in which a hydroxyl group is added to an epoxy, is observed to occur in systems that have stoichiometrically excess epoxy groups and when the cure temperature is greater than 150°C.<sup>2-5</sup> This reaction, also referred to as the OH-etherification reaction, introduces network defects in the form of additional crosslinks at intermediate positions along the polymer chain and also results

**Figure 1** Structure of Epon resins.

**Table II Cure and Postcure Schedules for the Epon Resins**

Resin	Cure Schedule	Postcure Schedule
825	2 h @ 100°, 1 h @ 140°C, 1 h @ 180°C	3 h @ 215°C
836	2 h @ 100°, 1 h @ 140°C	3 h @ 175°C
1001F	2 h @ 120°, 1 h @ 140°C	3 h @ 160°C
1002F	3 h @ 130°C	3 h @ 155°C
1004F	3 h @ 140°C	3 h @ 150°C

in dangling chains with unreacted epoxy and amine groups. In order to limit the extent of the OH-etherification reaction, all networks were synthesized with stoichiometric compositions and the temperature during the first stage of cure was maintained below 150°C.

Specimens for the mechanical tests were machined from the cured sheets. The machined specimens were then postcured according to the schedules listed in Table II. The postcure schedules, which yield complete conversion of the networks, were determined from Differential Scanning Calorimeter (DSC) studies using a Mettler DSC-30. Dynamic DSC studies were first conducted with stoichiometric mixtures of each Epon resin and *m*PDA to obtain estimates of the ultimate glass transition temperatures,  $T_{g\infty}$ , of the respective networks. Values of  $T_{g\infty}$  were then used to determine the isothermal postcure schedules for each network by postcuring the network at different temperatures for different times. The network  $T_g$  was used to track advancement of cure in the resins. A postcure for 3 h at 40°C above  $T_{g\infty}$  was determined to be sufficient to achieve the maximum  $T_g$  and the maximum possible conversion.

### Network Conversions

The extents of conversion of the fully cured networks were determined by Fourier Transform Infrared (FTIR) Spectroscopy. The FTIR analyses were performed with an IBM Instruments IR-32S FTIR spectrometer.

Stoichiometric mixtures of the Epon resin and *m*PDA were dissolved in methyl ethyl ketone (MEK) and the solution was cast onto NaCl cells. The solvent was evaporated under vacuum and the absorbance spectrum of the unreacted epoxy-amine mixture was first analyzed. The mixture was then cured, following a procedure identical to that used for the bulk resin sheets. After the postcure stage,

the absorbance spectrum of the network was analyzed again. The final conversion was calculated from the change in the peak area for the epoxy band (916  $\text{cm}^{-1}$ ), using the area under the band due to the C—C stretch of the bridge carbon atom (1184  $\text{cm}^{-1}$ ) as a reference. The expression for the conversion is,

$$X_{\text{epoxy}} = \frac{A_{e,\text{final}}A_{r,\text{initial}}}{A_{r,\text{final}}A_{e,\text{initial}}} \quad (1)$$

where  $A_e$  and  $A_r$  refer to the peak areas of the epoxy and the C—C bands and the subscripts initial and final correspond to the unreacted and the fully reacted systems.

### Crosslink Density

The networks were characterized in terms of the average mol wt between crosslinks,  $\bar{M}_c$ . The  $\bar{M}_c$  values were evaluated from the dynamical mechanical storage moduli assuming the validity of the theory of rubber elasticity.<sup>7</sup> The dynamic mechanical tests were conducted in torsion on a Rheometrics System IV Rheometer at a frequency of 1 Hz with 0.318 cm thick,  $1.27 \times 14 \text{ cm}^2$  specimens, under dynamic heating conditions of 5°C/min from -100° to 230°C. From the value of the storage modulus at a temperature of 40°C above the ultimate glass transition temperature of the network,  $\bar{M}_c$  was evaluated as:

$$\bar{M}_c = \frac{\phi \rho_T R T}{G'} \quad (2)$$

where  $\Phi$  is the front factor,  $T$  is the test temperature,  $\rho_T$  is the network density at the test temperature,  $R$  is the gas constant, and  $G'$  is the shear storage modulus. The front factor was assumed to be equal to unity in calculating  $\bar{M}_c$ .

Since the theory of rubber elasticity is strictly not valid for densely crosslinked networks, the  $\bar{M}_c$  values estimated from eq. (2) may incorporate some errors due to the non-Gaussian character of the short network chains of this study. Treloar<sup>7</sup> has developed expressions for the force-displacement characteristics of non-Gaussian network chains. For extension ratios less than 1.1 and for chains with five equivalent statistical links, this derivation suggests that eq. (2) can yield an underestimation of the true  $\bar{M}_c$  values by up to 23%; that is, the maximum errors involved in the application of eq. (2) to non-Gaussian chains can be 23%. For all the net-

works, the  $\bar{M}_c$  values were also determined independently from the reaction stoichiometry using a method developed by Lin and Bell.<sup>21</sup> These results are presented in a later section.

The network densities were determined by the density gradient technique on 0.5 cm wide and 0.5 to 1 cm long specimens machined from the fully cured sheets. Three specimens were used for each network. Ethanol and carbon tetrachloride were used as the column fluids and the density measurements were conducted in accordance with the procedure outlined in ASTM-D1505.<sup>8</sup>

The network bulk densities required in eq. (2) were calculated from the experimentally measured densities at room temperature and the network expansion coefficients in the glassy and the rubbery states using the relation:

$$\rho_T = \frac{\rho_{T_a}}{[1 + 3\alpha_g(T_{g_\infty} - T_a)] + [1 + 3\alpha_r(40)]} \quad (3)$$

where  $\rho_{T_a}$  is the density at temperature  $T_a$ ,  $\alpha_g$  is the linear expansion coefficient in the glassy state,  $\alpha_r$  is the linear expansion coefficient in the rubbery state,  $T_{g_\infty}$  is the network ultimate glass transition temperature, and  $T_a$  is the column temperature.

Linear expansion coefficients were measured on 0.5 cm cubes of each postcured network. The tests were conducted with a Perkin-Elmer 7 Series Thermal Analysis System. Measurements were conducted on two samples over a temperature range of 0° to 250°C, at 10°C/min. The expansion coefficients in the glassy and the rubbery states were determined from the slopes of the linear expansion-temperature plots above and below  $T_g$ .

## Specimens for Mechanical Tests

### Modulus

The glassy-state Young's modulus of the networks was determined using a three-point loading system. The specimens were machined according to the guidelines described in ASTM-D 790-87<sup>9</sup> and had widths of 1.27 cm and a support spans of 7.62 cm. The specimen thicknesses varied between 0.368 and 0.445 cm. All tests were conducted in a forced convection oven, mounted on an Instron Servohydraulic testing machine. Measurements at subambient temperatures were conducted using a controlled flow of liquid nitrogen. The temperature was regulated to within  $\pm 2^\circ\text{C}$  using electric heaters. All tests were performed at a constant displacement rate of 0.05

cm/min. The flexure modulus,  $E_f$ , was determined using the relation,

$$E_f = \frac{mL^3}{4Wh^3} \quad (4)$$

where  $m$  is the slope of the initial portion of the load-deflection plot,  $L$  is the support span,  $W$  is the specimen width, and  $h$  is the specimen thickness. The strains were restricted to 0.5%. At low strains, the flexure modulus is identical to the tensile modulus and thus  $E_f = E$ , where  $E$  is the tensile Young's modulus of the networks.<sup>10</sup>

## RESULTS AND DISCUSSION

### Conversions

Analysis of the infrared spectra of the uncured and the fully cured systems revealed only two noticeable changes: (i) a decrease in the N—H peak stretch from primary amines in the 3500–3400  $\text{cm}^{-1}$  range with a corresponding increase in the O—H peak due to secondary alcohols, and (ii) a decrease in the epoxy peak intensity at 916  $\text{cm}^{-1}$  with an associated increase in the peak intensities over the 1124–1087  $\text{cm}^{-1}$  interval due to C—O stretching vibration of saturated secondary alcohols. These changes are the result of the epoxy-amine addition reactions. The OH-etherification reaction generates aliphatic ethers with the CH—O—CH<sub>2</sub> groups. The IR-spectra of compounds with aliphatic ether groups typically exhibit a strong, asymmetric C—O—C stretching band around 1125  $\text{cm}^{-1}$ . Such a characteristic peak was not evident in the spectra of any of the networks studied.<sup>11</sup> The absence of this peak, therefore, suggests that the networks were formed predominantly by the epoxy-amine addition reactions.

Conversions of the Epon 825/*m*PDA through Epon 1002F/*m*PDA networks are listed in Table III. For Epon 1004F/*m*PDA, the changes in the epoxy peak intensity before and after the crosslinking reaction could not be determined accurately and the conversions are therefore not listed in Table III. For the networks of Epon 825, 836, and 1001F, the epoxy conversions are approximately 95%, while Epon 1002F/*m*PDA exhibits a conversion of 91%. A number of studies have shown that 100% conversion cannot be attained during the cure of stoichiometric mixtures of epoxy-amine systems, which form densely crosslinked networks.<sup>12–15</sup> At high con-

**Table III Network Conversions and Ultimate Glass Transition Temperatures**

Resin	825	836	1001F	1002F	1004F
Conversion (%)	95	96	95	91	—
$T_g^a$ (°C)	175	135	120	115	110
$T_g^b$ (°C)	165	135	118	116	113

<sup>a</sup> From dynamic DSC studies.

<sup>b</sup> From expansion coefficient studies.

versions, overall diffusion limitations and steric hindrances do not permit the interactions between spatially separated unreacted epoxy groups and amine hydrogens. The observed conversions for the Epon networks may therefore represent the topological limits for these systems.

### Glass Transition Temperatures

In this study, the increase in the network  $T_g$  with the extent of reaction was not monitored, but instead, only the ultimate glass transition temperatures of the fully reacted systems were determined. The results are listed in Table III and presented in Figure 2 as a plot of  $T_{g\infty}$  vs.  $\frac{1}{\bar{M}_n}$ , where  $\bar{M}_n$  is the number average mol wt of the prepolymers. From Figure 2, it is evident that  $T_{g\infty}$  varies linearly with  $\frac{1}{\bar{M}_n}$  over the range of mol wts studied. This behavior is similar to that observed by Banks and Ellis<sup>16</sup> for a series of epoxy resins cured with diaminodiphenyl methane (DDM).

Banks and Ellis<sup>16</sup> proposed a model to describe the glass transition temperature of fully cured networks formed by the addition reactions of linear prepolymers of different mol wts crosslinked with the same curing agent. The model is based on the assumptions of the additivity and the redistributivity of the network free volume. The  $T_{g\infty}$  of the network is expressed as:

$$T_{g\infty} = T_{g,1} + \frac{\zeta}{\bar{M}_n} \quad (5)$$

where  $T_{g,1}$  is the glass transition temperature of a polymer with an infinite mol wt with the same repeat unit as the prepolymer, and

$$\zeta = \frac{\gamma_2}{\gamma_1} \frac{M_R}{2} T_{g,2} \quad (6)$$

$\gamma_i$  in eq. (6) is equal to  $\frac{dX_i}{dT}$ , where  $X_i$  is the free volume contribution from species  $i$ , and the subscripts 1 and 2 refer to the prepolymer and the curing agent, respectively.  $\frac{\gamma_2}{\gamma_1}$  then characterizes the relative rates of increase  $X_2$  and  $X_1$  with temperature.  $M_R$  is the mol wt of the repeat unit in the prepolymer. For the epoxy resins of this study and those of Banks and Ellis, the structure of the prepolymer is as shown in Figure 1, and the repeat unit is the portion of the molecule within the square brackets.  $T_{g,2}$  is the glass transition temperature of a hypothetical network formed by the end-linking of the curing agent molecules.

Banks and Ellis<sup>16</sup> studied networks with  $\bar{M}_n$  values ranging from 355 g/mol to 4955 g/mol and, from a plot of  $T_{g\infty}$  vs.  $\frac{1}{\bar{M}_n}$ , determined an intercept of 365 K and a slope of 17300 g-K/mol. For the epoxy-*m*PDA networks of this study, the intercept is 365.7 K, and the slope is 28,436 g-K/mol. The values of the intercept in the two studies are similar and are also similar to the glass transition temperature of the polyhydroxyether of bisphenol-A (PHEBPA). The glass transition temperature of PHEBPA of mol wt 45,000 g/mol has been reported to be 373 K.<sup>17</sup> The repeat unit in the structure of polyhydroxyether of bisphenol-A is identical to that in the Epon resins of this study and those of Banks and Ellis, and a

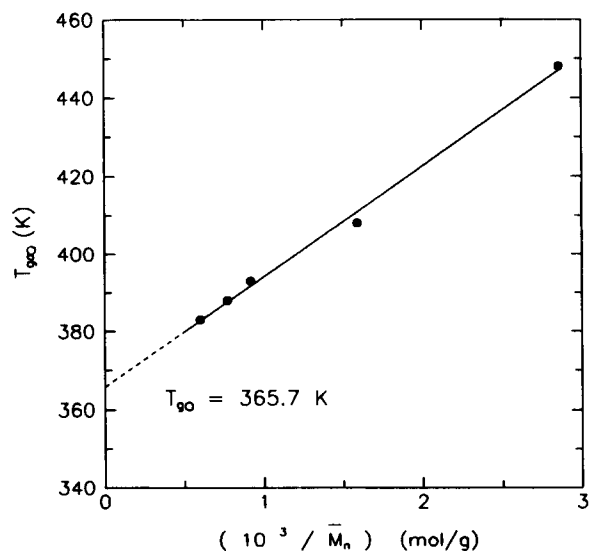


**Figure 2** Variation in ultimate glass transition temperature with reciprocal of average prepolymer mol wt for a series of Epon resins cured with *m*PDA.

similarity in  $T_{g,1}$  provides evidence in support of the physical interpretation of  $T_{g,1}$ .

The slope of the  $T_{g\infty}$  vs.  $\frac{1}{M_n}$  plot for the networks of this study is greater than that reported by Banks and Ellis.<sup>16</sup>  $M_R$  and  $\gamma_1$  are identical in both studies and a greater slope, therefore, merely reflects greater values of the product ( $\gamma_2 T_{g,2}$ ) for *m*PDA as compared to DDM.  $T_{g,2}$  for *m*PDA is expected to be greater than for DDM, since a hypothetical network formed solely from the *m*PDA units is likely to be stiffer than one formed using DDM. This may be the reason for the steeper slope observed for the networks cured with *m*PDA.

### Dynamic Mechanical Properties and Mol Wts between Crosslinks

The results of the dynamic mechanical studies are presented in Figures 3 to 7. The drop in the storage modulus, and the corresponding maximum in the loss modulus curves of the polymers, are due to the transitions associated with increases in internal freedom, such as long range segmental motions at the primary ( $\alpha$ ) transition and localized motions of chain segments or side-groups at the secondary ( $\beta$ ) transition temperature.

In Figures 3–7, the  $\alpha$ - and the  $\beta$ -transition peaks are seen in the loss modulus curves for all the networks studied. The  $\alpha$ -transition peaks occur at 177, 147, 129, 130, and 120°C for the networks of Epon 825, 836, 1001F, 1002F, and 1004F, respectively. The

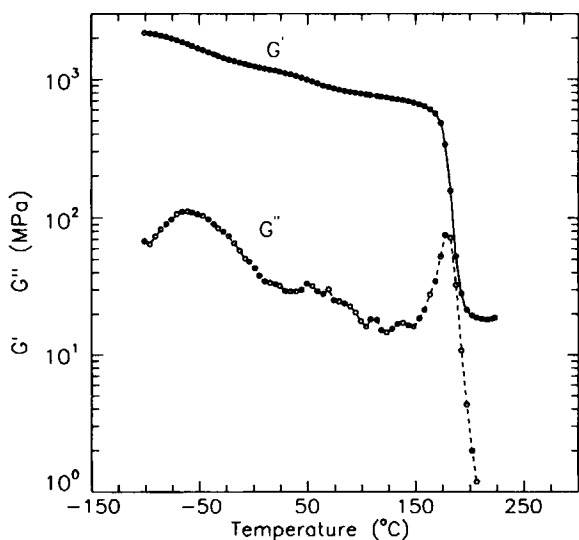


**Figure 3** Dynamic mechanical storage and loss moduli of Epon 825/*m*PDA at 1 Hz.

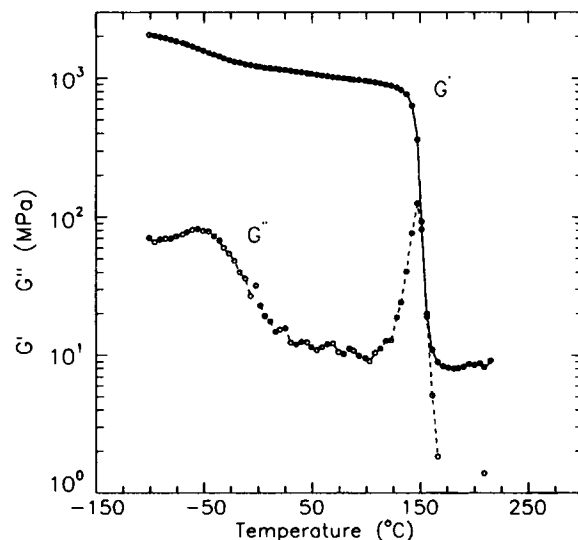


**Figure 4** Dynamic mechanical storage and loss moduli of Epon 836/*m*PDA at 1 Hz.

results are listed in Table IV. The peak temperatures are 5 to 10°C greater than the  $T_{g\infty}$  values determined by dynamic DSC studies (see Table III). The apparent peak shifts to higher temperatures may merely be due to a different definition of glass transition employed for the dynamic mechanical studies. In DSC studies, the glass transition is defined by the temperature at the onset of the endothermic deflection of the DSC trace, whereas in dynamic mechanical studies, the loss modulus peak temperature, which defines the glass transition, corresponds to the mid-point in the transition from a glassy to a rubbery state. Consequently,  $T_g$  values, determined

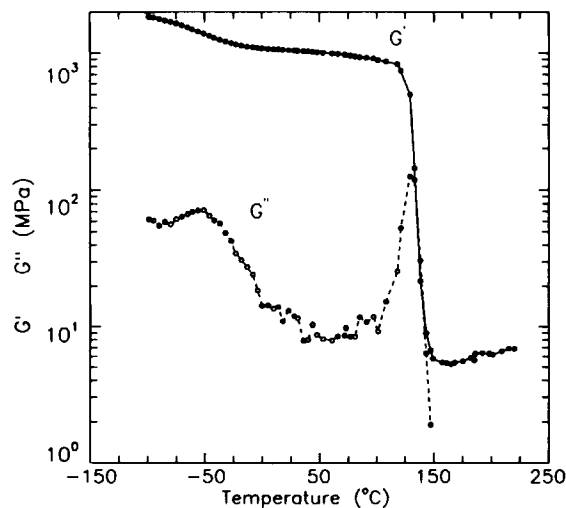


**Figure 5** Dynamic mechanical storage and loss moduli of Epon 1001F/*m*PDA at 1 Hz.

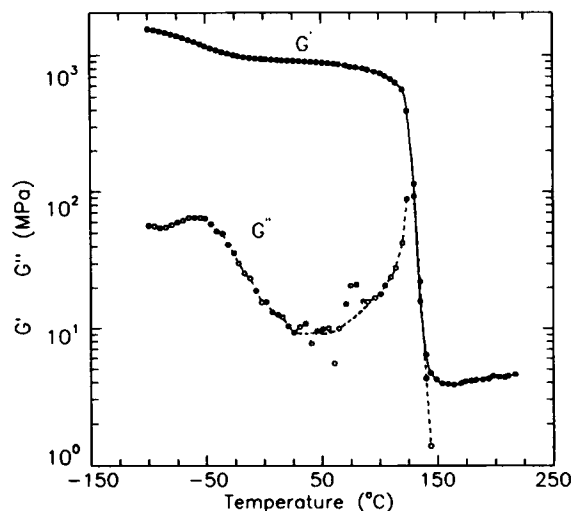


**Figure 6** Dynamic mechanical storage and loss moduli of Epon 1002F/mPDA at 1 Hz.

from the dynamic mechanical studies, may be higher than the  $T_{g_{cc}}$  values obtained from the DSC studies.

Unlike the primary transitions, the  $\beta$ -transition peaks for all the networks occur over a narrow tem-

perature range of  $-53^\circ$  to  $-60^\circ\text{C}$ . The molecular origin of the  $\beta$ -transition in crosslinked epoxy resins has been attributed to the glyceryl group in the network structure.<sup>18-20</sup>

The average mol wt between crosslinks for the Epon networks was determined from the dynamic mechanical storage moduli at  $(T_{g_{cc}} + 40)^\circ\text{C}$ , using eq. (2). Values of  $\bar{M}_c$  are listed in Table V.

The mol wt between crosslinks was also estimated from the reaction stoichiometry and the final network conversions. Lin and Bell<sup>21</sup> have described a technique for the estimation of the effective mol wt between crosslinks,  $M_{c_{eff}}$ , from the reaction stoichiometry. This method incorporates the effects of partially reacted epoxy groups and amine hydrogens, which result in ineffective crosslinks or dangling chains. For a difunctional epoxy reacted with a tetrafunctional amine, the effective mol wt between crosslinks is:

$$M_{c_{eff}} = \frac{\text{Total mol wt} - \text{mol wt of dangling ends}}{\text{Number of effective chains}} \quad (7)$$

which can be written as

$$M_{c_{eff}} = \frac{aMW_a + bMW_e - \frac{(P + E)(aMW_a + bMW_e)}{\frac{3}{2}(2a - P - S) + \frac{(P + E)}{2}}}{\frac{3}{2}(2a - P - S) - \frac{3}{2}(P + E)} \quad (8)$$

where  $a$  and  $b$  are the initial number of moles of amine and epoxy;  $MW_a$  and  $MW_e$  are the mol wts of the amine and the epoxy, and  $E$ ,  $P$ , and  $S$  are the concentrations of unreacted epoxy, primary amine, and secondary amine groups, respectively. In the absence of OH-etherification, the concentration of unreacted epoxy groups can be related to the concentration of primary and secondary amine groups, which have reacted by

$$E = 2b - (2a - P) - (2a - P - S) \quad (9)$$

For initial stoichiometric compositions of epoxy groups to amine hydrogens,  $P$  can be assumed to be zero since the epoxy-primary amine reaction is reported to be nearly ten times faster than the epoxy-secondary amine reaction and, when most of the epoxy groups have reacted, the concentration of primary amine groups will tend to zero. Thus, for  $P \rightarrow 0$ ,

$$\begin{aligned} S &= E = (1 - X_n)b \\ &= (1 - X_n)2a \end{aligned} \quad (10)$$

where  $X_n$  is the epoxy conversion.  $M_{c_{eff}}$  is then:

$$M_{c_{eff}} = \frac{M_T - \frac{(1 - X_n)4M_T}{[3 - 4(1 - X_n)]}}{3 - 12(1 - X_n)} \quad (11)$$

where

$$M_T = \left( MW_a + \frac{b}{a} MW_e \right) \quad (12)$$

Values of the effective mol wt between crosslinks are listed in Table V. The experimentally determined  $\bar{M}_c$  values agree within 15 to 18% with the

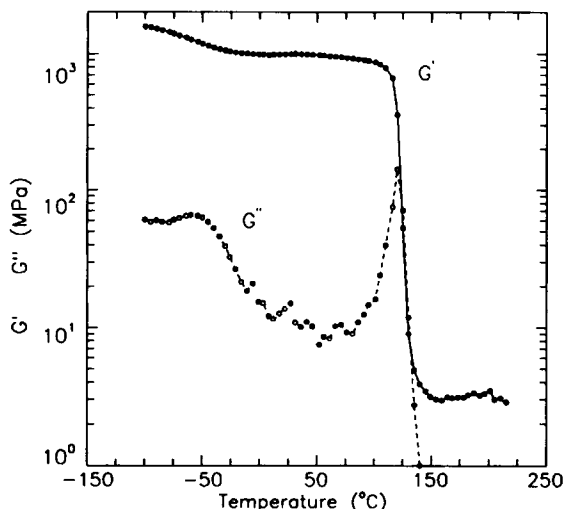


**Figure 7** Dynamic mechanical storage and loss moduli of Epon 1004F/*m*PDA at 1 Hz.

$M_{c,eff}$  values calculated from the stoichiometry of the reaction system.

### Expansion Coefficients

The results of the expansion coefficient studies are listed in Table VI and are shown in Figure 8. In the glassy state, all the networks exhibit similar coefficients of expansion; however, in the rubbery state, the expansion coefficients increase with an increase in the mol wt between crosslinks.

The glass transition temperatures determined from the intersection of the linear portions of the expansion curves above and below  $T_g$  are also listed in Table III. Except for Epon 825/*m*PDA, which exhibits a slightly lower  $T_g$ , the  $T_g$  values are in good agreement with those determined by dynamic DSC studies.

### Densities

If the density differences between a prepolymer and a curing agent are not large, the bulk densities of

**Table IV** Primary- and Secondary-Transition Peak Temperatures from Dynamic Mechanical Loss Modulus Studies

Network	$T_\beta$ (°C)	$T_\alpha$ (°C)
Epon 825/ <i>m</i> PDA	-61	177
Epon 836/ <i>m</i> PDA	-56	147
Epon 1001F/ <i>m</i> PDA	-53	129
Epon 1002F/ <i>m</i> PDA	-55	130
Epon 1004F/ <i>m</i> PDA	-60	120

**Table V** Average Mol Wt Between Crosslinks

Network	825	836	1001F	1002F	1004F
$\bar{M}_c$ (g/mol)	257	527	774	1043	1286
$M_{c,eff}$ (g/mol)	313	512	885	1215	1486

$\bar{M}_c$ , experimental (from dynamic mechanical storage modulus).  
 $M_{c,eff}$ , from Stoichiometry.

the crosslinked networks increase with an increase in the crosslink density, or alternatively, the specific volumes decrease as the crosslink density is increased. The densities of the Epon resins vary from 1.155 g/cm<sup>3</sup> for Epon 825 to 1.222 g/cm<sup>3</sup> for Epon 1004F,<sup>22</sup> while the density of *m*PDA is 1.139 g/cm<sup>3</sup>.<sup>23</sup>

Nielsen<sup>24</sup> has referenced a number of studies where the network specific volume is observed to decrease linearly with an increase in the crosslink density, and has proposed an empirical relationship between the network specific volume and the concentration of crosslinks. The relationship is:

$$\bar{v} = \bar{v}_o - kN_c \quad (13)$$

where  $\bar{v}$  is the specific volume of the crosslinked polymer,  $\bar{v}_o$  is the specific volume of the uncrosslinked polymer,  $N_c$  is the number of moles of curing agent per gram of network, and  $k$  is a constant.

In this study, since all the networks were formed from stoichiometric compositions of the epoxy and amine, values of  $N_c$  were estimated as

$$N_c = \frac{EW_a}{MW_a} \frac{1}{(EEW + EW_a)} \quad (14)$$

where  $EW_a$  is the equivalent weight of amine and  $MW_a$  is the mol wt of the amine. A plot of  $\bar{v}$  as a function of  $N_c$  is shown in Figure 9. A linear rela-

**Table VI** Expansion Coefficients and Densities of the Networks

Network	$\alpha_g \times 10^{-4}$ (°C <sup>-1</sup> )	$\alpha_r \times 10^{-4}$ (°C <sup>-1</sup> )	$\rho_0$ (g/cm <sup>3</sup> )
Epon 825/ <i>m</i> PDA	0.66	1.83	1.2114
Epon 836/ <i>m</i> PDA	0.67	1.96	1.2032
Epon 1001F/ <i>m</i> PDA	0.67	2.02	1.1992
Epon 1002F/ <i>m</i> PDA	0.67	2.04	1.1975
Epon 1004F/ <i>m</i> PDA	0.68	2.07	1.1969

$\alpha_g$ , expansion coefficient in the glassy state.  
 $\alpha_r$ , expansion coefficient in the rubbery state.  
 $\rho_0$ , network density at room temperature.



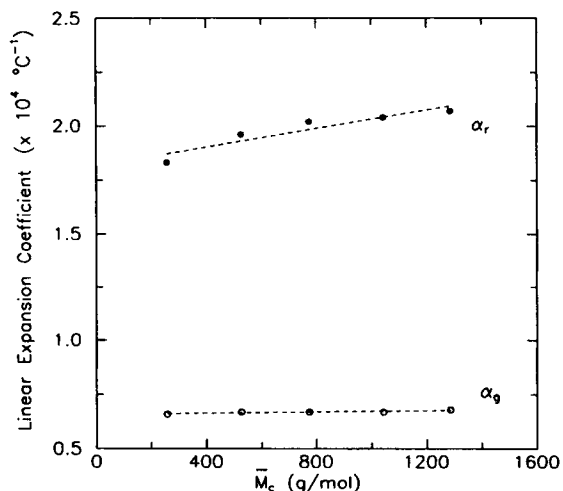


**Figure 8** Variation in linear expansion coefficient with the network average mol wt between crosslinks ( $\alpha_r$ , rubbery state;  $\alpha_g$ , glassy state).

relationship is observed with a slope of  $0.0107 \text{ cm}^3/(\text{mol amine})$  and  $\bar{v}_o$  of  $0.839 \text{ cm}^3/\text{g}$ .

**Modulus**

The temperature dependence of the glassy-state moduli of all the networks is shown in Figure 10. The modulus varies linearly with temperature with different slopes above  $-25^\circ\text{C}$  and below  $-50^\circ\text{C}$ . Above  $-25^\circ\text{C}$ , both the magnitude and the temperature dependence of the moduli of all the networks are similar.

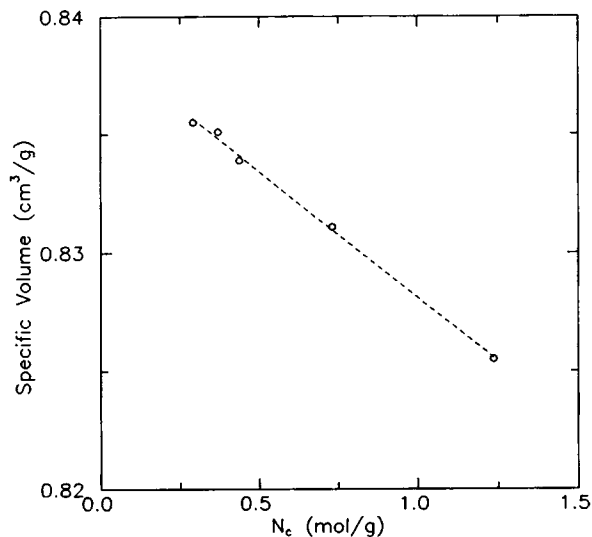


**Figure 9** Variation in network specific volume with curing agent concentration for the resins of Epon 825, 836, 1001F, 1002F, and 1004F.

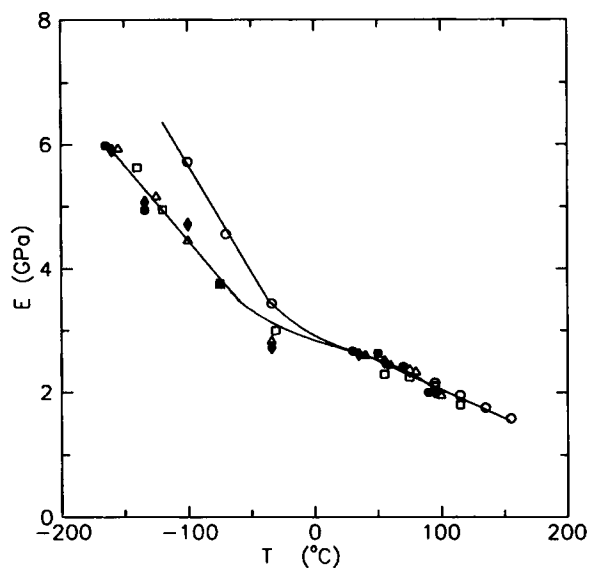


**Figure 10** Temperature dependence of flexure moduli for a series of Epon resins cured with *mPDA*.

To illustrate the invariance of the modulus with the network structure, modulus values at room temperature ( $25^\circ\text{C}$ ) are plotted as a function of the average mol wt between crosslinks in Figure 11. Within the limits of experimental error, which are of the order of  $\pm 10\%$ , the modulus does not exhibit any network structure dependence over a five-fold variation in  $\bar{M}_c$ . Similar results have been reported by Nielsen,<sup>24</sup> Bell,<sup>2</sup> Labana et al.,<sup>25</sup> Selby and Miller,<sup>26</sup>

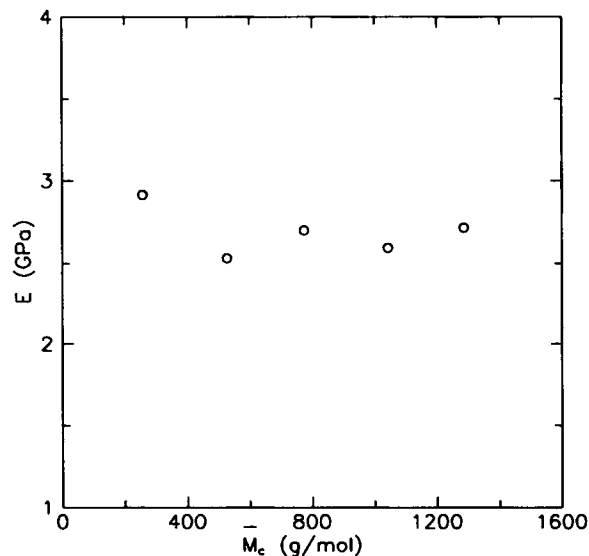


**Figure 11** Variation in flexure modulus at  $25^\circ\text{C}$  with the average mol wt between crosslinks for a series of Epon resins cured with *mPDA*.

and Kim et al.<sup>27</sup> for the room temperature moduli of networks of different crosslink densities.

For the modulus data below  $-50^{\circ}\text{C}$ , two differences are apparent in comparison with the data above  $-25^{\circ}\text{C}$ . First, the slope of the modulus-temperature plot is steeper below  $-50^{\circ}\text{C}$  than it is above it. Second, at all temperatures below  $-50^{\circ}\text{C}$ , the modulus of Epon 825/*m*PDA is greater than those of the other networks, while at temperatures above  $-25^{\circ}\text{C}$  the moduli are independent of the crosslink density.

The change in slope of the modulus-temperature plot occurs over the same temperature interval as the  $\beta$ -transition of the networks. A steeper modulus-temperature behavior below the  $\beta$ -transition temperature,  $T_{\beta}$ , may be a consequence of the fact that the motions of the glyceryl groups are frozen below  $T_{\beta}$ .

Similar relations between molecular relaxations and macroscopic mechanical properties have been observed in impact and yield stress studies. For example, a correlation between impact strength and mechanical losses was observed by Vincent.<sup>28</sup> Impact tests on several thermoplastic polymers over a wide temperature range showed pronounced peaks in the brittle impact strength at temperatures closely matching the peaks in the dynamic mechanical loss tangent. Also, Bauwens-Crowet et al.<sup>29</sup> observed that the yield stress-temperature plot of polycarbonate (PC) exhibited a discontinuity near the  $\beta$ -transition temperature of PC. This behavior is similar in nature to the modulus-temperature behavior observed in this study and reflects the influence of the molecular structure on the macroscopic mechanical properties.

## SUMMARY AND CONCLUSIONS

The results of the experimental studies with the Epon resins/*m*PDA systems suggest that, with suitably controlled curing conditions, nearly ideal networks can be synthesized from a difunctional epoxy and a tetrafunctional amine. These networks can then be used as model systems to study the network structure influence on mechanical properties.

The results of the infrared spectroscopic studies provide confirmation of the fact that the networks were formed primarily by the epoxy-amine addition reactions. A peak corresponding to the C—O—C stretch of aliphatic ethers, resulting from the OH-etherification reaction, was not detected in the spectra of any of the networks. The networks were characterized in terms of the average mol wt between

crosslinks,  $\bar{M}_c$ , calculated from experimental dynamic mechanical shear moduli and assuming the validity of the theory of rubber elasticity.  $\bar{M}_c$  values were also predicted from the reaction stoichiometry and the predicted values were in fair agreement with those calculated experimentally, suggesting that even though the rubber elasticity theory is strictly inapplicable to densely crosslinked networks, this technique can be adopted to characterize dense networks.

The elastic modulus, being a low strain mechanical property, did not exhibit any  $\bar{M}_c$  dependence above room temperature. But the temperature dependence of the modulus of all the networks was influenced by the localized  $\beta$ -relaxations in the epoxy chains. Dynamic mechanical studies showed a  $\beta$ -transition peak over a narrow temperature interval of  $-57$  to  $-61^{\circ}\text{C}$  and modulus-temperature plot exhibited a discontinuity over a similar temperature interval.

The authors appreciate the cooperation of Mr. Paul Jones at the Shell Development Company for a generous supply of the Epon resins and Dr. J. T. Gotro at the IBM Corporation for the dynamic mechanical and the expansion coefficient studies.

## REFERENCES

1. ASTM-D 1652-87, *Epoxy Content of Epoxy Resins*, Annual Book of ASTM Standards, ASTM, Philadelphia, 1988.
2. J. P. Bell, *J. Appl. Polym. Sci.*, **14**, 1901 (1970).
3. H. C. Anderson, *SPE J.*, **16**, 1241 (1960).
4. E. F. Oleinik, *Adv. Polym. Sci.*, **80**, 49 (1986).
5. K. Dusek, in *Rubber-Modified Thermoset Resins*, C. K. Riew and J. K. Gillham, Eds., *Adv. Chem. Ser.*, **208**, 3 (1984).
6. L. Schechter, J. Wynstra, and R. Kurkky, *Ind. Eng. Chem.*, **48**(1), 94 (1956).
7. L. R. G. Treloar, *The Physics of Rubber Elasticity*, Clarendon, Oxford, 1975.
8. ASTM-D 1505-87, *Density of Plastics by the Density Gradient Technique*, Annual Book of ASTM Standards, ASTM, Philadelphia, 1988.
9. ASTM-D 790-87, *Flexural Properties of Unreinforced and Reinforced Plastics*, Annual Book of ASTM Standards, ASTM, Philadelphia, 1988.
10. L. A. Carlsson and R. Byron Pipes, *Experimental Characterization of Advanced Composite Materials*, Prentice-Hall, NJ, 1987.
11. U. M. Vakil, *Analysis of Structure-Mechanical Property Relations in Crosslinked Epoxies*, Ph.D. Dissertation, Syracuse University (1990).

12. J. P. Bell, *J. Polym. Sci.*, **8**(A-2), 417 (1970).
13. M. A. Acitelli, R. B. Prime, and E. Sacher, *Polymer*, **12**, 335 (1971).
14. E. F. Oleinik, *Pure Appl. Chem.*, **53**, 1567 (1981).
15. B. A. Rozenberg, *Adv. Polym. Sci.*, **75**, 113 (1986).
16. L. Banks and B. Ellis, *Polymer*, **23**, 1466 (1982).
17. N. H. Reinking, A. E. Barnabeo, and W. F. Hale, *J. Appl. Polym. Sci.*, **7**, 2135 (1963).
18. O. Delatycki, J. C. Shaw, and J. G. Williams, *J. Polym. Sci.*, **7**, 753 (1969).
19. G. A. Pogany, *Polymer*, **11**, 66 (1970).
20. J. G. Williams, *J. Appl. Polym. Sci.*, **23**, 3433 (1979).
21. C. J. Lin and J. P. Bell, *J. Appl. Polym. Sci.*, **16**, 1721, (1972).
22. Shell Development Co., Technical Bulletin, 1989.
23. J. A. Dean, Ed., *Lange's Handbook of Chemistry*, McGraw-Hill, New York, 1979.
24. L. E. Nielsen, *J. Macromol. Sci. Revs. Macromol. Chem.*, **C3**(1), 69 (1969).
25. S. S. Labana, S. Newman, and A. J. Chompff, in *Polymer Networks, Structure, and Mechanical Properties*, A. J. Chompff and S. Newman, Eds., Plenum, New York, 1971.
26. K. Selby and L. E. Miller, *J. Mater. Sci.*, **10**, 12 (1975).
27. S. L. Kim, M. D. Skibo, J. A. Manson, R. W. Hertzberg, and J. Janiszewski, *Polym. Eng. Sci.*, **18**, 1093 (1978).
28. P. I. Vincent, *Polymer*, **15**, 111 (1974).
29. C. Bauwens-Crowet, J.-C. Bauwens, and G. Homes, *J. Mater. Sci.*, **7**, 176 (1972).
30. U. M. Vakil and G. C. Martin, *Fracture and Yield Behavior of Crosslinked Epoxies*, submitted *J. Mater. Sci.*

Received May 1, 1991

Accepted December 12, 1991